SEISMIC INTERACTION OF SOIL-PIPELINE SYSTEM THROUGH THE FRICTIONAL INTERFACE

T. Akiyoshi (I)
K. Fuchida (II)
Presenting Author: T. Akiyoshi

SUMMARY

This paper presents the seismic interaction analysis between soil and buried pipelines. The solutions of imperfectly bonded soil-pipeline system are obtained in closed form based on the frictional slippage of the main pipe and the wave propagation in the far field. The numerical considerations are made on the mean square response not only of the strain and the joint expansion of the main pipe, but the end stress of the branch pipes, subjected to the recorded strong motions. Recommendations are made to densely distribute the joints for preventing the failures by slippage during earthquakes.

INTRODUCTION

In almost all of the existing investigations on the earthquake response of buried pipelines, the slip between pipe and surrounding soil has been overlooked. It is now known through bench-scale and field experiments that the slip phenomenon plays an important role during earthquakes. Numerous analytical modelings of very small vibrational amplitudes of the shear force acting at the soil-pipe interface were reported in the literature [for example, Toki and Takada(Ref. 1), Ugai (Refs. 2 and 3) and Parnes(Ref. 4)]. However, no serious analytical modeling of large vibrational amplitudes for such systems is possible until a good model of slipping is adopted.

This paper offers the concept of large vibrational amplitudes in dealing with the interaction of imperfectly bonded soil-pipe system during earthquakes. The friction at the interface is assumed to be of Coulomb mechanism by a viscous friction model having a viscous coefficient developed by Miller (Ref. 5) and Akiyoshi (Ref. 6). Analysis is first made for steady-harmonic earthquakes (=plane P-and S-waves), and the slip displacement is represented in closed form which involves some earthquake, soil and pipe parameters. Further the periodically jointed pipelines are analyzed by replacing them with the statically equivalent linear and uniform ones, and then the branch pipes elastically connected both to the main pipes and the structures are investigated. Those harmonic solutions are extended to the seismic response of buried pipes subjected to recorded strong motions, decomposing them into discrete spectral amplitudes by the fast Fourier transform.

GENERAL FORMULATION AND SOLUTION

When an earthquake propagates toward a pipeline as shown in Fig. 1,

---

(I) Professor of Earthquake Engineering, Kumamoto Univ., Kumamoto, Japan
(II) Research Associate of Concrete Structure, Yatsushiro College of Technology, Kumamoto.

part of the incident wave will be reflected at the surface of the pipeline. Thus the wave in soil is generally represented by superposing the incident and outgoing waves.

Axial Vibration of Soil-Pipeline System

For the axial vibration of the soil-pipe system the radial and axial displacements may be sufficient to analyze the respective interaction. Using the solution of the soil displacement w_z by Ugai (Ref. 3) the shear stress τ_{rz} at the interface is obtained as (Ref. 6)

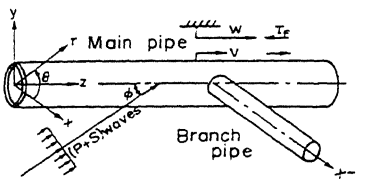

Fig. 1 Geometry of problem

$$\tau_{rz}|_{r=r_0} = \mu \frac{\partial w_z}{\partial r}\Big|_{r=r_0} = -(\alpha_1 w_1 + \alpha_2 w_2) \qquad (1)$$

where w_1, w_2 = displacement amplitudes of incident and reflected P-waves respectively, $k_l = \omega/v_l$ = wave number of P-wave, ω = circular frequency, v_l = velocity of P-wave, ϕ = incident angle to main pipe axis, $i = \sqrt{(-1)}$, $H_0^{(2)}(\ )$, $H_1^{(2)}(\ )$ = Hankel functions of order zero and one of the second kind, $k_s = \omega/v_s$ = wave number of S-wave, v_s = velocity of S-wave, $\mu = G$ = shear modulus of soil, $q_l = k_l \sin\phi$, $q_s = k_s h_s$, $h_s = \sqrt{[1 - (v_s/v_l)^2 \cos^2\phi]}$, $\alpha_1 = \mu k_l \sin\phi \, J_1(q_l r_0)/J_0(q_l r_0)$, $J_0(\ )$, $J_1(\ )$ = Bessel functions, and

$$\alpha_2 = \frac{\rho\omega^2}{F(r_0)}, \quad F(r) = \frac{k_l^2 \cos^2\phi}{q_l} \frac{H_0^{(2)}(q_l r)}{H_1^{(2)}(q_l r_0)} + \frac{q_s H_0^{(2)}(q_s r)}{H_1^{(2)}(q_s r_0)} \qquad (2)$$

In the above expressions α_2 in eq. (2) has been called "resistance factor" of soil by Nogami and Novak (Ref. 7).

Formulation of Slippage

When the slip at the soil-pipe interface occurs, the frictional stress τ_F equals the boundary sress τ_{rz} in eq. (1):

$$\tau_F = \tau_{rz}|_{r=r_0} \qquad (3)$$

For a broad class of frictional models, the frictional stress τ_F depends only on the slip displacement u and the velocity amplitude $\dot{u} = du/dt$ which can be replaced with an equivalent system [Caughey (Ref. 8), Miller (Ref. 5)]. Thus if Coulomb friction as shown in Fig. 2 is assumed at the soil-pipe interface, τ_F is approximately represented by

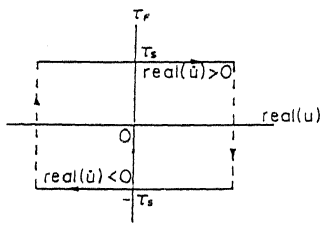

Fig. 2 Frictional stress-slip displacement relation in Coulomb friction

$$\tau_F = \frac{4\tau_s}{\pi\omega U}\dot{u} \qquad (4)$$

where τ_s = slip stress, U = real amplitude of the slip displacement u.

Under the steady-harmonic excitation the slip displacement u will take the following expression:

$$u = Ue^{i(\omega t - k_l z\cos\phi - \phi_U)} \qquad (5)$$

where ϕ_U = phase difference of the slip displacement u.

Axial Interaction

The governing equation of axially vibrating pipe is written by

$$m \frac{\partial^2 v_z}{\partial t^2} = ES \frac{\partial^2 v_z}{\partial z^2} + 2\pi r_0 \tau_{rz}|_{r=r_0} \tag{6}$$

where v_z = axial displacement of pipe, m = unit length mass of pipe, E = Young's modulus of pipe, S = cross sectional area of pipe, r_0 = radius of pipe and τ_{rz} = shear stress acting on the interface.

Now define the slip displacement u by the difference between the soil displacement w_z and the pipe one v_z;

$$u = w_z - v_z \tag{7}$$

Then substitution of u, v_z, w_z and τ_{rz} of eq. (1) into eq. (6) leads to the complex equation in terms of U and ϕ_U. Therefore separation of the equation into the real and imaginary parts gives the system of equations which may be solved as

$$U = -\frac{4\tau_s}{\pi} s_2 + \sqrt{\left[\{(1-\alpha_1 s_1)^2+\alpha_1^2 s_2^2\}|w'_{z1}|^2 - (\frac{4\tau_s}{\pi})^2 (\frac{2\pi r_0}{M_0}+s_1)^2\right]} \tag{8}$$

only if $|w'_{z1}| > w_{cr}$, and otherwise $U = 0$ where

$$w_{cr} = \frac{4\tau_s}{\pi} \sqrt{\left[(\frac{2\pi r_0}{M_0}+s_1)^2 + s_2^2\right]} / \sqrt{\left[(1-\alpha_1 s_1)^2 + \alpha_1^2 s_2^2\right]} \tag{9}$$

where $M_0 = -m\omega^2 + ESk_l^2 \cos^2\phi$, $w_{z1} = w_1 \cos\phi$, a, b = respectively real and imaginary part of α_2, and $s_1 = a/(a^2+b^2)$, $s_2 = b/(a^2+b^2)$. Hence

$$v_z = H_{z1}(\omega)\, w_1 \cos\phi\, e^{i(\omega t - k_l z \cos\phi)} \tag{10}$$

where $H_{z1}(\omega)$ = frequency response function of axially vibrating pipe to P-wave which yields

$$H_{z1}(\omega) = 2\pi r_0 (\alpha_2 - \alpha_1) i\frac{4\tau_s}{\pi} / \left[M_0 U \alpha_2 + i\frac{4\tau_s}{\pi}(M_0 + 2\pi r_0 \alpha_2)\right] \tag{11}$$

Estimation of Joint Expansions of Main Pipes

Consider a long pipeline which consists of finite length pipes and periodically arranged joints whose axial stiffness are represented with $k_p = ES/l$ and k_j respectively (E, S, l = Young's modulus, cross sectional area and length of the pipe). Then the equivalent axial stiffness $k' = E'S/l$ will satisfy the relation

$$\frac{1}{k'} = \frac{1}{k_p} + \frac{1}{k_j} \quad \text{or} \quad \frac{v'_p}{v_p} = \sqrt{\left(1 - \frac{1}{1+k_j/k_p}\right)} \tag{12}$$

where E', v'_p = apparent Young's modulus and wave velocity of the equivalent pipe. For a ductile cast iron pipe the relation $k_j/k_p = l/36$ (unit of l = meters) is available (Ref. 9).

If some obstacles such as buildings or T-joints prevent the smooth propagation through the pipelines, the maximum joint expansion d may be estimated by the sum of the slip displacement d_s of the single pipe and the relative displacement d_j of the joint;

$$d = d_s + d_j$$

$$= P_1(\omega)\, w_1 e^{i\omega t} + P_2(\omega)\, w_2 e^{i\omega t} \qquad (13)$$

where FRF of the joints to P-wave takes the form

$$P_1(\omega) = (\alpha_2-\alpha_1)M_0U/[M_0U\alpha_2+i\frac{4\tau_s}{\pi}(M_0+2\pi r_0\alpha_1)]\cos\phi[e^{-ik_l l\cos\phi}-1]$$
$$+[H_{z1}(\omega)\cos\phi+ir_0k_l\cos\phi H_{x1}(\omega)\sin\phi][e^{-ik_l e\cos\phi}-1] \qquad (14)$$

and FRF to S-wave may also take almost the similar form in which e = effective length of joint.

Branch Pipe Response

Consider a branch pipe of the length l' and the radius r_0' in which the both ends are elastically and perpendicularly connected to the main pipe and the structure. When the earthquake waves propagate toward the main pipe with the incident angle ϕ, the branch pipe will also be subjected to the same waves with the incident angle $\psi = 90° - \phi$ as shown in Fig. 3. Then the equation of the transverse motion v_z of the branch pipe is written by

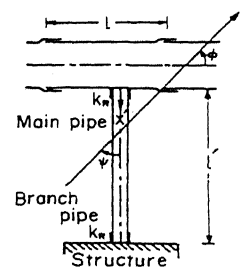

Fig. 3 Geometry of main and branch pipes

$$EI'\frac{d^4v_z}{dx'^4} + \frac{d}{dx'}(N'\frac{dv_z}{dx'}) = p_z' \qquad (15)$$

where I', N' = geometrical moment of inertia and axial force of the branch pipe respectively, and p_z' = lateral earth pressure to the branch pipe which is generally represented as $p_z' = k_z(w_1\sin\phi - v_z')$, k_z = earth pressure per unit displacement (Ref. 6).

Since the lateral earth pressure to such slender pipe is very large compared with the pipe stiffness EI', the movement of the branch pipe is restricted except for the both ends. Thus the solution of eq. (15) to P-wave, which is valid close to the pipe ends, will be approximately represented by

$$v_z = \frac{w_1\cos\phi(1-H_{z1})}{(\lambda_1-\lambda_2)(\frac{k_R}{EI'}+\lambda_1+\lambda_2)}[(\frac{k_R}{EI'}+\lambda_2)\lambda_2 e^{-\lambda_1 x'}-(\frac{k_R}{EI'}+\lambda_1)\lambda_1 e^{-\lambda_2 x'}] \qquad (16)$$

where

$$\lambda_1,\ \lambda_2 = \sqrt{\{-\frac{N_1}{2EI'} \pm \sqrt{(\frac{N_1}{2EI'})^2 - \frac{K_1}{EI'}}\}},$$

k_R = rotational stiffness of the T-joint.

NUMERICAL RESULTS

Numerical computations are conducted for the root mean square (RMS) response of ductile cast iron (DCI) pipes buried in the elastic soil. The standard values of the parameters of earthquakes, pipes and soils used for computations are the incident angle $\phi = 45°$, the shear wave velocity of soil, $v_s = 200$ m/s, ratio of P-to S-wave velocity, $v_l/v_s = 2$,

ratio of slip stress to shear modulus of soil, $\tau_s/G = 10^{-4}$, radius of main pipe, $r_0 = 0.3\ m$, wave velocity of pipe, $v_p = 4000\ m/s$, nondimensional mass ratio $m = 0.5$, and $I/Sr_0^2 = 0.5$.

El Centro (1940) earthquakes are used as the reference P-and S-waves having RMS accelerations of 0.5 m/s^2 whose Fourier spectra are plotted in Fig. 4.

Appropriate choice of Fourier decomposition number N is required in advance of RMS analysis. Fig. 5 denotes that N = 1024 is sufficient to represent the discrete spectral displacements at the low frequency range. The diagram also shows $|w_{z1}| < w_{cr}$ which means no slip at any frequency.

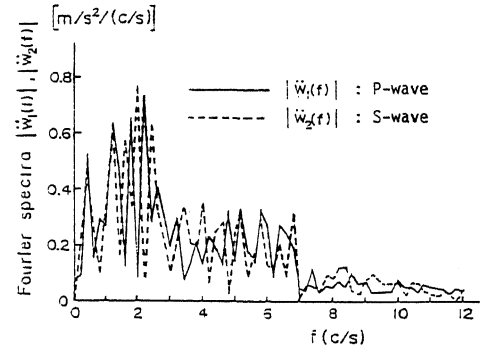

Fig. 4 Fourier spectra of P-and S-waves for computation

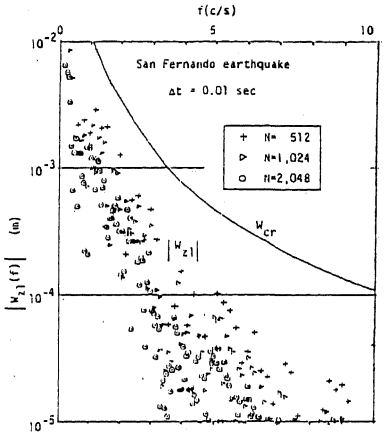

Fig. 5 Displacement Fourier spectra (San Fernando earthquake)

Fig. 6 is the plot of RMS strain of the main pipe versus incident angle ϕ, subjected to the reference earthquakes (P-and S-waves) of the RMS = 0.5 m/s^2. This plot denotes that the slip is caused mainly by P-wave because the slip arises for small incident angle with decreasing slip stress.

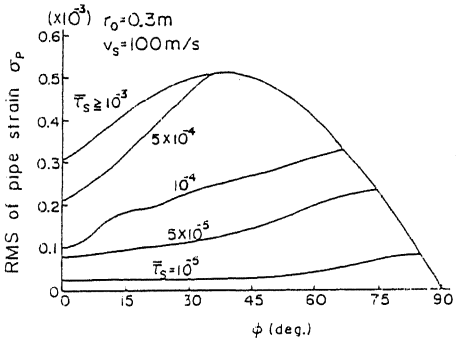

Fig. 6 RMS of pipe strain versus incident angle

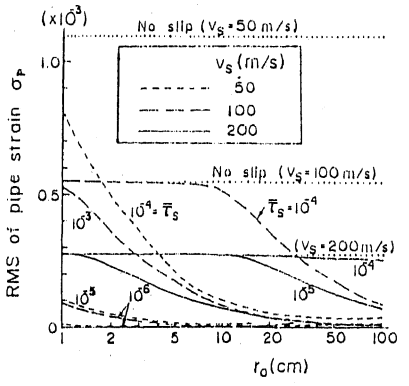

Fig. 7 RMS of pipe strain versus radius

Fig. 7 is the diagram showing the effect of the pipe radius r_0 on RMS strain σ_p of the ductile cast iron (DCI) pipe. The pipe strain is small for small slip stress, soft soil (small v_s) and large diameter pipe. In such case the earthquake damage of the pipes will be released, but the joints must absorb the slippage.

Fig. 8 is the diagram denoting the effect of S-wave velocity v_s of the soil on RMS strains of DCI pipes for $r_0 = 0.3\ m$. Deceasing v_s which is equivalent to decreasing soil stiffness increases the possibility of the slip of the pipes. Therefore it follows that v_s and τ_s have the equivalent effect on the slip of pipes.

In Fig. 9 RMS of the pipe strain is plotted versus RMS of the soil strain subjected to the accelerograms of the duration of $T = 20.48$ seconds which have been recorded on the ground surface in Japan and U.S.A. It is shown that the small-diameter pipes follow the surrounding soil unless the boundary shear stress yields. This means that the slip works effectively for lowering the strain of the large-diameter and stiff pipe.

Fig. 10 is the diagram of the joint expansions of the joint-pipe systems versus the apparent wave velocity v_p' of the pipes and the pipe length l. It is noted that RMS joint expansion σ_d decreases with decreasing pipe length l, and is depressed under $1\ mm$ unless the slip occurs. Thus the dense distribution of the joints results in lowering the stiffness of the pipeline systems and restricting the joint expansion below an allowable values.

Fig. 11 shows the stress distributions of branch pipes in which the stress concentration dominates close to the end for thin branch pipe and loosens for thick pipe.

Effect of rotational stiffness K_R of the branch pipe on the end stress σ_j is plotted in Fig. 12 in which the solid and dotted lines denote the stress of the branch pipes at $x' = 0$ and $x' = l'/10$ respectively. Stress-concentrated position moves to the end of the branch pipe with hard clamping (large K_R) at the T-joints.

It is also shown in Fig. 13 that the soft soil (small v_s) causes the slip of the main pipe and therefore induces the remarkable stress increment of the branch pipe.

CONCLUSIONS

The effect of slippage of buried pipes during earthquakes on the pipe strain, the joint expansions and the end stress of the branch pipes have been theoretically investigated, using the existing solutions of elastic waves in the far field. Results obtained are summarized as follows:

(1) Slip consideration at the soil-pipe interface enables to eliminate the restriction of the small amplitude assumed in the conventional seismic wave propagation analyses.
(2) Most of slips begin with small incident angle. Therefore the maximum slip is expected when P-wave propagates along the pipe axis. Further the slip in general tends to occur for large-diameter pipe, large stiffness ratio of pipe to soil, small slip stress, and large power of earthquakes.
(3) For small-diameter (slender) pipes, interaction effect on pipe strain increases with the diameter, but is very small. Hence the pipe

strain is almost equal to the soil one unless the slip occurs. If the slip occurs the pipe strain is restricted below the soil strain during earthquakes.
(4) Dense distributions of the joints in the pipeline systems lower the stiffness and release the stress concentration at the joints.
(5) Soft soil, small diameter and hard clamping of the T-joints concentrate the stress at the ends of the branch pipes.

REFERENCES

1. Toki, K. and S. Takada(1974), "Earthquake Response Analysis of Undergound Tubular Structure," Part 2, Bull. Disas. Prev. Resear. Instit., Kyoto Univ., Vol. 221, pp.107-125.
2. Ugai, K.(1978), "Dynamic Analysis of Underground Pipelines under the Condition of Axial Sliding," Proc. JSCE, No. 272, pp.27-37(in Japanese).
3. Ugai, K.(1979), "A Theoretical Study on the Dynamic Modulus of Earth Reaction for Buried Pipe," J. JSSMFE, Vol. 21, No. 4, pp.93-102(in Japanese).
4. Parnes, R. and P. Weidlinger(1981), "Dynamic Interaction of an Embedded Cylindrical Rod under Axial Harmonic Forces," Int. J. Solids Struct., Vol. 17, pp.903-913.
5. Miller, R. K.(1977), "An Approximate Method of Analysis of the Transmission of Elastic Waves through a Frictional Boundary," J. App. Mech., ASME, Vol. 44, No. 4, pp.652-656.
6. Akiyoshi, T. and K. Fuchida(1982), "Soil-Pipeline Interaction through a Frictional Interface during Earthquakes," Proc. Conf. Soil Dyn. and Earthq. Eng., Southampton, pp.495-511.
7. Nogami, T. and M. Novak(1976), "Soil-Pile Interaction in Vertical Vibration," Int. J. Earthq. Eng. and Struct. Dyn., Vol. 4, pp.277-293.
8. Caughey, T. K.(1963), "Equivalent Linearization Techniques," J. Acout. Soc. America, Vol. 35, No. 11, pp.1706-1711.
9. Takada, S.(1980), "Dynamic Response Analysis of PVC and Ductile Iron Pipelines," Proc. Pressure Ves. and Piping Conf., ASME, pp.23-32.

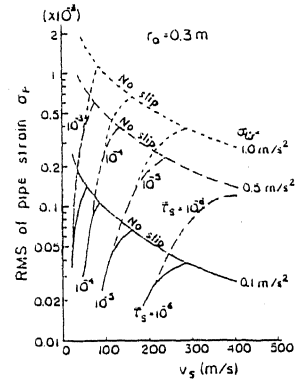

Fig. 8 RMS of pipe strain versus velocity of soil

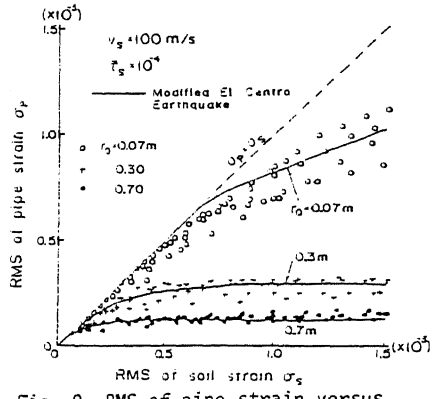

Fig. 9 RMS of pipe strain versus RMS of soil strain

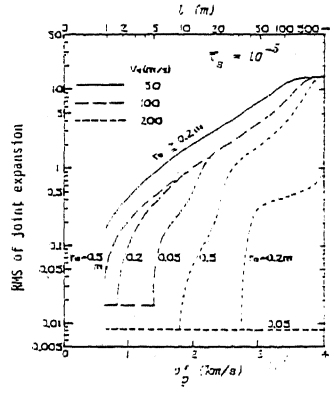

Fig. 10 RMS of joint expansion versus pipe length

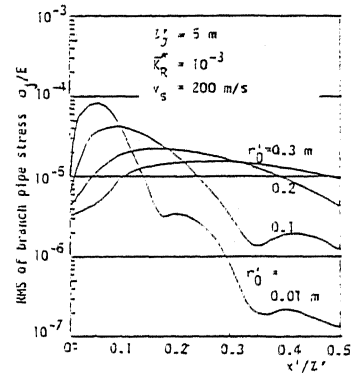

Fig. 11 Stress distribution of branch pipes

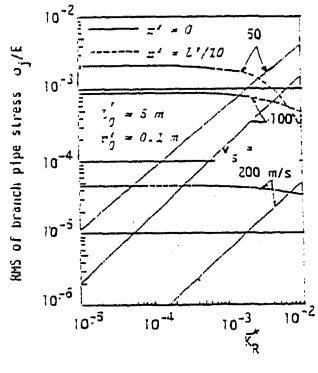

Fig. 12 Effect of rotational stiffness on the end stress of branch pipes

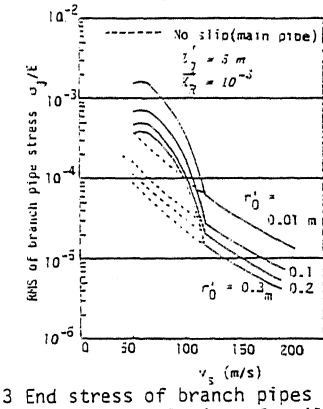

Fig. 13 End stress of branch pipes versus shear wave velocity of soil